Quantum Electronics **47** (9) 853–859 (2017)
©2017 Kvantovaya Elektronika and Turpion Ltd

VUV SPECTROSCOPY

https://doi.org/10.1070/QEL16392

Versatile and compact wide-range VUV spectrometer for quantitative measurements

A.P. Shevelko

Abstract. **Main parameters of a new scheme of a compact VUV grazing incidence spectrometer based on a plane amplitude diffraction grating are considered. The spectrometer will allow simultaneous detection of spectra at the +1st order diffraction edge with a sufficiently high ($\lambda/\delta\lambda \sim 150$) spectral resolution and in the –1st order with a moderate resolution ($\lambda/\delta\lambda \sim 15-30$), but in a very wide (5–200 nm) spectral range. The use of such a spectrometer is promising for measuring the absolute radiation yield in these spectral regions, which is necessary for the diagnostics and control of plasma radiation sources, including those intended for projection EUV nanolithography.**

Keywords: *VUV spectroscopy and radiometry, plasma diagnostics, VUV spectrometers, EUV nanolithography.*

1. Introduction

Recently, vacuum ultraviolet (VUV) and soft X-ray spectral ranges have attracted special attention in connection with the need to develop new radiation sources for various practical applications (microscopy of biological objects in the 'water window', nanolithography, etc.) and plasma diagnostics [1]. In many cases, quantitative (absolute) measurements of intensities in spectra, both in individual spectral lines and in given narrow and wide spectral intervals, acquire special significance. These measurements are particularly important for projection EUV (Extreme Ultra Violet) nanolithography – one of the most promising technologies for mass production of integrated circuits with element sizes less than 20 nm (see, for example, reviews [2–6] and references therein). The most important component of this technology is the use of intensive sources of EUV radiation. Strict requirements imposed on these sources include such main parameters as the total radiation power and the conversion efficiency at working wavelengths (λ_0 = 13.5 and 6.6 nm). This requires measurements of the absolute radiation yield not only at working wavelengths, but also in a wide spectral range [2–4]. The latter are necessary for determining the energy spectral composition (balance) of radiation falling into the optical system of the lithograph. In addition, control and diagnostics of radiation sources require monitoring of the absolute spectrum in real time. All this allows us to formulate general requirements to spectral devices for studying VUV radiation sources for nanolithography: the possibility of performing absolute measurements in a wide spectral range and with a low spectral resolution; good spectral resolution in a narrow, working range; recording of spectra in real time; and a compact size for integration into technological or experimental facilities.

A.P. Shevelko P.N. Lebedev Physical Institute, Russian Academy of Sciences, Leninsky prosp. 53, 119991 Moscow, Russia; e-mail: apshev51@gmail.com

Received 4 April 2017; revision received 5 June 2017
Kvantovaya Elektronika **47** (9) 853–859 (2017)
Translated by I.A. Ulitkin

Carrying out absolute measurements is one of the topical problems of VUV spectroscopy. In this range, all substances possess large absorption coefficients varying sharply as functions of the wavelength, which greatly affects the reflectivity of diffraction gratings and mirrors, the sensitivity of detectors, and other characteristics of devices. In addition, the coverage of the entire VUV spectral range requires, as a rule, several spectral instruments, while their calibration should rely on the use of special VU reflectometers or synchrotron radiation. This greatly complicates the calibration procedure. The issue of using absolute radiation detectors is also a priority. The application of scintillation detectors, thermocouples, pin-diodes requires the use of monochromators, but in this case the monitoring of the entire spectrum is impossible. The situation has significantly changed for the better with the appearance of backside-illuminated CCD arrays and matrices. They are real-time detectors, have known absolute sensitivity in a wide VUV spectral range, high sensitivity, good signal-to-noise ratio and wide dynamic range. However, when using these detectors, some additional requirements to the measurement procedure arise: it is necessary to fit the entire spectrum at the detector length (usually ~30 mm) and to project it onto a flat sensitive CCD surface.

One of the ways to solve the problem of performing absolute measurements in a wide spectral range is to use a transmission grating spectrometer (TGS) (see, for example, Refs [7–13] and monograph [14]). The grating efficiency is usually determined theoretically, and the use of an absolutely calibrated radiation detector allows, in principle, absolute measurements. However, the employment of transmission gratings has disadvantages. Thus, the width of the spectral range is in contradiction with the spectral resolution. To expand the spectral range at a required spectral resolution, several gratings are necessary [11, 12]. Due to the complex composition of the grating material and deviation from the ideal geometry of the grooves (bars), there sometimes appear great difficulties in calculating the grating transmission. This leads to the need for additional calibration of TGSs with synchrotron radiation sources, especially in the long-wavelength (λ > 100 nm) spectral range [13].

To date, numerous schemes of spectrometers and their modifications with reflection gratings have been developed (see, e.g., review [15] and monographs [16–18]). In the VUV region of the spectrum, the focusing schemes of the spectro-

meters use mainly concave grazing incidence gratings. Such schemes allow a high spectral resolution to be obtained; however, the possibilities of using them for solving the assigned tasks are severely limited. Focusing spectrometers have, as a rule, a curved focal surface (for example, the Rowland circle), which makes it impossible to employ CCD detectors. Flat-field spectrometers using gratings with a variable period of the grooves are applicable in a limited spectral range. The presence of higher orders of reflection and relatively large dimensions also pertain to the disadvantages of focusing spectrometers. In this connection, it is of interest to use plane diffraction gratings in non-focusing schemes. As early as the beginning of the last century, plane gratings were used in X-ray spectrographs [19–21]. The registration of the spectrum formed by a plane grating in non-focusing schemes allows the use of CCD detectors, and in addition, plane gratings can be easily ruled with the required profile of the grooves. For this reason, we propose a new solution in this paper – the use of a plane amplitude grazing incidence grating for recording VUV spectra. As will be shown below, the asymmetry of reflection in ±1st diffraction orders allows one to simultaneously record VUV radiation in a wide spectral range and to have a sufficiently high spectral resolution in a narrow range. The paper describes and discusses the main parameters of the scheme of such a compact VUV grazing incidence spectrometer based on a plane amplitude grating (AGS). Since an AGS is an alternative to a TGS, a brief description of the latter is given for comparing the parameters of both spectrometers.

2. Transmission grating spectrometer

A transmission grating, or a slit grating [16], is a periodic structure with absorbing grooves (bars), alternating with transparent slits. In this case, the diffraction pattern is observed in the transmitted light (Fig. 1a). The basic scheme of a simplest TGS is shown in Fig. 2: the radiation under investigation, passing through the entrance slit, is incident on a plane diffraction grating, and the diffraction spectrum is detected by a radiation detector. Usually, the entrance slit is spatially combined with the grating.

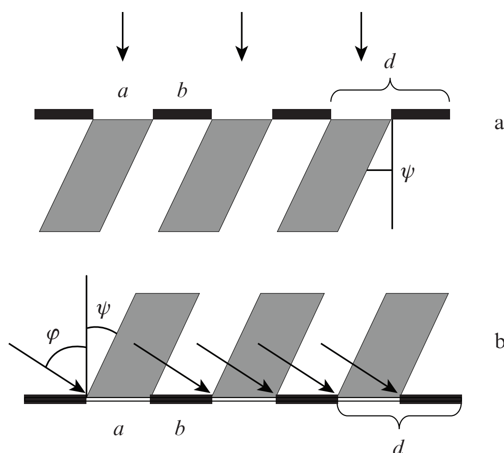

Figure 1. Schemes of (a) transmission and (b) reflection diffraction gratings; a is the width of the transmissive (reflecting) part, b is the width of the absorbing (non-reflecting) part, $d = (a + b)$ is the grating period, φ is the angle of incidence, ψ is the diffraction angle, the arrows indicate incident radiation, gray areas show diffracted radiation.

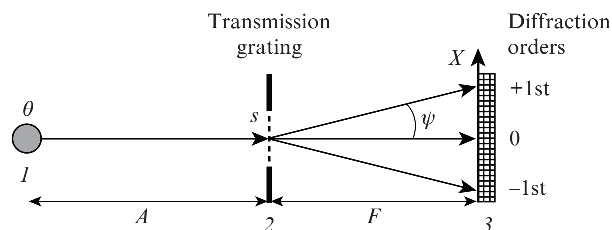

Figure 2. Scheme of a TGS: (*1*) radiation source; (*2*) entrance slit and transmission grating; (*3*) radiation detector; θ is the size of the source; s is the width of the entrance slit; A is the distance from the source to the input slit; F is the distance from the grating to the registration plane.

An important condition for the use of a transmission grating for calibration purposes is the equality of the ratio of the widths of its transmissive (a) and absorbing (b) parts to unity (Fig. 1a). In this case, radiation is completely suppressed in even diffraction orders and the radiation intensity in odd higher orders decreases substantially [7, 16]. This makes it possible to considerably simplify the theoretical calculations of the grating transmission at different wavelengths, and the use of an absolutely calibrated detector allows one, in principle, to carry out absolute measurements in a wide spectral range.

Since the incidence angle of the radiation on the grating is $\varphi = 0$, the grating equation is simplified:

$$d \sin\psi = n\lambda, \tag{1}$$

where ψ is the diffraction angle; d is the grating period; and n is the diffraction order. Here and below, for simplicity, we will consider only the first orders of diffraction, $n = \pm 1$. The expression for the inverse linear dispersion D^{-1} is obtained by differentiating equation (1):

$$D^{-1} = \frac{d\lambda}{dX} = \frac{d\cos\psi}{F}, \tag{2}$$

where F is the distance from the grating to the registration plane. The inverse dispersion D^{-1} for small angles ψ at which TGS operates is a constant and does not depend on ψ or λ:

$$D^{-1} = \frac{d\lambda}{dX} = \frac{d}{F}. \tag{3}$$

The spectral resolution $\delta\lambda$ of the spectrometer is determined by the following parameters: the number of grating grooves participating in diffraction, the width of the image of the monochromatic line in the registration plane for point and extended sources, and the width of the instrument function of the detector used. Let us consider them in more detail.

The spectral resolving power is determined by the number N of slits participating in the diffraction:

$$\frac{\lambda}{\delta\lambda_0} = N = \frac{s}{d}, \tag{4}$$

and the spectral resolution

$$\delta\lambda_0 = \frac{\lambda}{N} = \frac{\lambda d}{s}. \tag{5}$$

The width of the source image in the monochromatic light X in the registration plane is determined by the known expressions for a one-dimensional pinhole camera, and the corre-

sponding spectral resolution is $\delta\lambda = D^{-1}X$. For a point source (Fig. 3a)

$$X_1 = s\frac{A+F}{A}, \quad (6)$$

where A is the distance from the source to the entrance slit (grating). The spectral resolution is expressed as

$$\delta\lambda_1 = \frac{d}{F}s\frac{A+F}{A} = \frac{d}{F}s\left(1+\frac{F}{A}\right). \quad (7)$$

If $A \gg F$, this expression is simplified:

$$\delta\lambda_1 = s\frac{d}{F} = sD^{-1}. \quad (8)$$

For an extended source of size θ (Fig. 3b)

$$X_2 = \theta\frac{F}{A}, \quad (9)$$

$$\delta\lambda_2 = d\frac{\theta}{A} = f\gamma_2, \quad (10)$$

where $\gamma_2 = \theta/A$ is the angular size of the source.

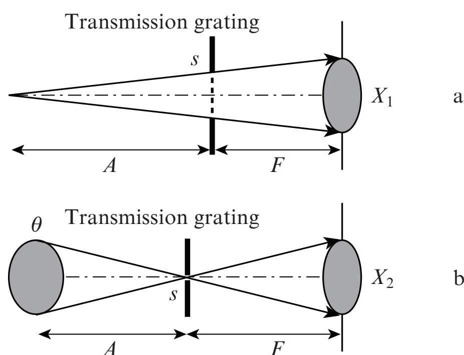

Figure 3. Image in the monochromatic light in the TGS registration plane of (a) point and (b) extended sources.

The spectral resolution, determined by the width of the instrument function ΔX of the radiation detector, has the form

$$\delta\lambda_d = \Delta X D^{-1} = \Delta X\frac{d}{F}. \quad (11)$$

In the case of using CCD arrays or matrices, ΔX is usually equal to the total width of two or three pixels.

The resulting spectral resolution can be determined by the expression

$$\delta\lambda = \sqrt{(\delta\lambda_0)^2 + (\delta\lambda_1)^2 + (\delta\lambda_2)^2 + (\delta\lambda_d)^2}\,. \quad (12)$$

For all the factors determining the spectral resolution, $\delta\lambda \backsim d$, and for its increase, it is necessary to decrease the grating period. However, in this case, the inverse dispersion also decreases, and hence a narrower portion of the spectrum is detected by a detector with a fixed width of the sensitive part. Therefore, it can be ascertained that in a TGS the width of the detected spectral range is in contradiction with the spectral resolution.

3. Amplitude reflection grating spectrometer

An amplitude reflection grating is a flat mirror surface with non-reflective grooves [16] (see Fig. 1b). A grating of this type is more durable than a transmission grating and is less time-consuming: its production requires less than half of the technological process necessary for fabricating transmission gratings [9].

The flat relief of the amplitude grating with a small roughness of the reflecting surface made of a known material and having a certain thickness of the reflective part of the groove allows one to reliably calculate the reflection coefficient. In addition, the installation of a grating in a grazing incidence scheme makes it possible to simplify the theoretical calculations of the reflection coefficient and to increase it in the short-wavelength range of the spectrum. As for the transmission grating, in order to completely suppress the reflection in even diffraction orders, it is necessary to satisfy the relation $a:b = 1:1$ (see Fig. 1b).

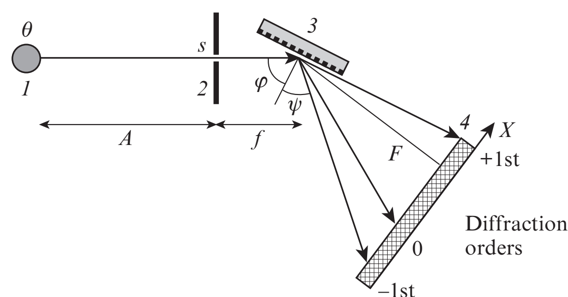

Figure 4. AGS scheme with amplitude reflection grating: (*1*) radiation source; (*2*) entrance slit; (*3*) grating; (*4*) radiation detector; f is the distance from the entrance slit to the center of the grating.

The scheme of the amplitude reflection grating spectrometer is shown in Fig. 4. Here the following numbering of diffraction orders is used: +1st order when $|\psi| > |\varphi|$ and –1st order when $|\psi| < |\varphi|$ [16]. We write the grating equation for the ±1 orders in the form

$$\sin\psi - \sin\varphi = n\lambda/d. \quad (13)$$

The inverse dispersion is

$$D^{-1} = \frac{d\lambda}{dX} = \frac{d\cos\psi}{F}. \quad (14)$$

Since the AGS operates at large diffraction angles ψ, the dependence of D^{-1} on $\cos\psi$ becomes significant (Fig. 5).

The spectral resolution $\delta\lambda$ is determined by the same parameters as for the TGS: the number N of grooves in the grating at which diffraction occurs, the width of the source image in the monochromatic light in the registration plane for point and extended sources and the width of the instrument function of the detector used.

The spectral resolving power, determined by the number N of the grooves, is as follows:

$$\frac{\lambda}{\delta\lambda_0} = N = \frac{s}{d\cos\varphi}, \quad (15)$$

and the spectral resolution

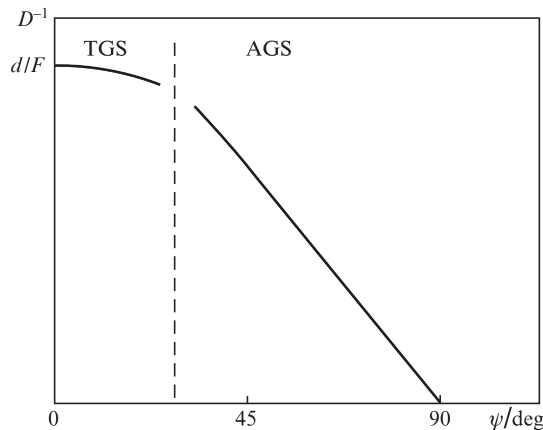

Figure 5. Dependences of the inverse dispersion D^{-1} on the diffraction angle ψ for a TGS and an AGS. The dashed line conditionally separates the regions of angles ψ.

$$\delta\lambda_0 = \frac{\lambda}{N} = \lambda\frac{d\cos\varphi}{s}. \tag{16}$$

The presence of the factor $\cos\varphi$ in (16), which is small for the grazing incidence scheme, makes it possible to significantly improve the filling of the grating and increase the number N of the grooves that ensure diffraction.

Consider the image size in the monochromatic light in the registration plane in cases of point and extended sources. Suppose that a beam with divergence γ falls on the grating, and a beam with divergence β is reflected (Fig. 6). In the monochromatic light, the image size is

$$X = \beta(r + F) = \beta r + \beta F, \tag{17}$$

where r is the distance from the point of convergence of the rays at an angle β to the centre of the grating. The value of βr is determined by the projection l_1 or l_2 of the width l of the illuminated part of the grating in directions perpendicular to the axes of the incident or reflected beams. These quantities are determined by the divergence angle γ of the radiation incident on the grating. We have:

$$l_2 = l_1\frac{\cos\psi}{\cos\varphi} = ml_1 = \beta r, \tag{18}$$

$$l = \frac{l_1}{\cos\varphi}, \tag{19}$$

where $m = \cos\psi/\cos\varphi$ is the grating angle magnification.

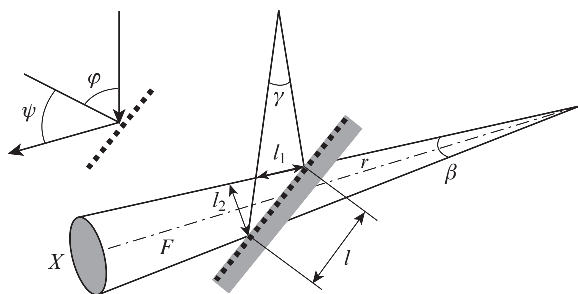

Figure 6. Scheme of the formation of a monochromatic source image in the registration plane for an AGS.

The relation between the angle β and the angle γ is found from the grating equation (13) when the angles $\varphi \pm \gamma/2$ and $\psi \pm \beta/2$ are substituted into it. After simple transformations, we obtain

$$\sin\frac{\gamma}{2} = \sin\frac{\beta}{2}\frac{\cos\psi}{\cos\varphi} \tag{20}$$

or, due to the smallness of the angles γ and β,

$$\gamma = \beta\frac{\cos\psi}{\cos\varphi}. \tag{21}$$

Thus, the angles γ and β are related with each other through the grating angle magnification:

$$\frac{\gamma}{\beta} = \frac{\cos\psi}{\cos\varphi} = \frac{l_2}{l_1}. \tag{22}$$

Finally, from (17) we have

$$X = l_1 m + \frac{\gamma}{m}F. \tag{23}$$

The divergence γ for a point source is determined by the angular width of the entrance slit, $\gamma_1 = s/A$, and for an extended source by its angular size $\gamma_2 = \theta/A$.

For a point source, $\gamma_1 = s/A$, $l_1 = s$, and the expression for X_1 has the form:

$$X_1 = s\frac{\cos\psi}{\cos\varphi} + \frac{sF}{A}\frac{\cos\varphi}{\cos\psi}. \tag{24}$$

The spectral resolution

$$\delta\lambda_1 = \frac{sd}{F}\frac{\cos^2\psi}{\cos\varphi} + \frac{sd}{A}\cos\varphi. \tag{25}$$

It is easy to show that for all practical cases with $A \gg F$ the second term in (25) can be neglected. It becomes significant only at diffraction angles ψ close to 90°, when the first term is close to zero because of the factor $\cos^2\psi$. However, in this limit, the resulting resolution is determined by other factors. For the first term we have

$$\delta\lambda_1 = \frac{sd}{F}\frac{\cos^2\psi}{\cos\varphi} = sD^{-1}m, \tag{26}$$

that is, the resolution is determined by the width of the entrance slit, inverse dispersion and grating angle magnification.

For an extended source with an angular size $\gamma_2 = \theta/A$, we have from (23)

$$X_2 = \theta\frac{f}{A}\frac{\cos\psi}{\cos\varphi} + F\frac{\theta}{A}\frac{\cos\varphi}{\cos\psi} \approx \frac{F\theta}{A}\frac{\cos\varphi}{\cos\psi}, \tag{27}$$

since for $f \ll F$ and not too small diffraction angles ψ we can take into account only the second term (f is the distance from the entrance slit to the grating centre). Then, the spectral resolution

$$\delta\lambda_2 = \frac{d\theta}{A}\cos\varphi = \gamma_2 d\cos\varphi. \tag{28}$$

The spectral resolution, determined by the instrument function ΔX of the radiation detector, has the from

$$\delta\lambda_{\rm d} = \Delta X D^{-1} = \Delta X \frac{d}{F}\cos\psi. \qquad (29)$$

The resulting spectral resolution, as in the case of a TGS, is determined by expression (12). The results of calculating the values of $\delta\lambda$ for $d = 3$ μm, $\varphi = 84.5°$, $\theta = 0.4$ mm, $s = 50$ μm, $A = 1000$ mm, $F = 60$ mm, $\Delta X = 75$ μm are shown in Fig. 7. Figure 8 shows the wavelength dependence of the resulting spectral resolving power of the AGS.

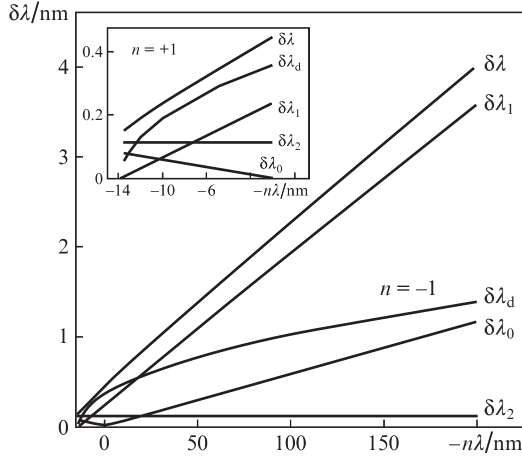

Figure 7. Dependences of the calculated values of $\delta\lambda$ of the AGS usage, determined by various factors ($n = +1$ and $n = -1$), on $n\lambda$.

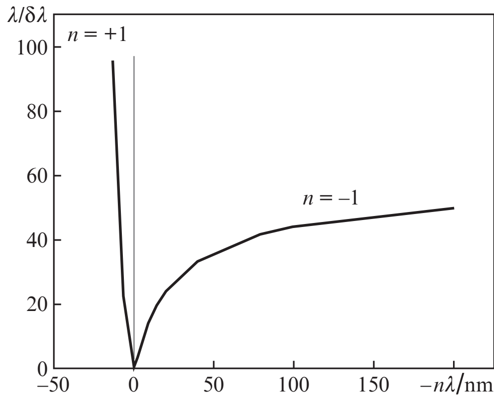

Figure 8. Dependence of the AGS resulting spectral resolving power on $n\lambda$.

Let us compare the TGS and AGS parameters (Table 1). In a TGS, use is made of an incidence angle $\varphi = 0$ and small diffraction angles ψ. The inverse dispersion is $D^{-1} = d\lambda/(dX) = d/F \approx$ const and almost does not depend on the diffraction angle ψ and the wavelength λ (Fig. 5). The spectra in the +1st and –1st diffraction orders are absolutely symmetric. The AGS uses small grazing angles (or large angles of incidence, $\varphi \approx 80°–90°$) and large diffraction angles, up to $\psi \approx 90°$. The inverse dispersion $D^{-1} = d\lambda/(dX) = d\cos\psi/F$ strongly depends on $\cos\psi$ and, consequently, on the wavelength λ (Fig. 5). The spectra in the +1st and –1st orders are strongly asymmetric. In a TGS, the inverse dispersion D^{-1} and the spectral resolutions $\delta\lambda$, due to various factors, are independent of the angles φ and ψ (Table 1). In an AGS, due to the grazing angle of incidence on the grating, the expressions for the inverse dispersion D^{-1} and the spectral resolution $\delta\lambda$ contain the factors ($\cos\varphi$, $\cos\psi \ll 1$), which depend on the incidence angles φ and the diffraction angle ψ (Table 1). This is an advantage of an AGS, because it allows the spectral resolution to be significantly enhanced. Note that all the formulas for the AGS in Table 1 at $\varphi \approx \psi \approx 0°$ ($\cos\varphi \approx 1$ and $\cos\psi \approx 1$) are transferred to formulas for the TGS.

Table 1. Spectral parameters of a TGS and an AGS.

Spectrometer	D^{-1}	$\delta\lambda_0$	$\delta\lambda_1$	$\delta\lambda_2$	$\delta\lambda_{\rm d}$
TGS	$\frac{d}{F}$	$\frac{\lambda d}{s}$	$s\frac{d}{F}$	$d\frac{\theta}{A}$	$\Delta X\frac{d}{F}$
AGS	$\frac{d\cos\psi}{F}$	$\lambda\frac{d\cos\varphi}{s}$	$\frac{sd}{F}\frac{\cos^2\psi}{\cos\varphi}$	$\frac{d\theta}{A}\cos\varphi$	$\Delta X\frac{d}{F}\cos\psi$

Another interesting feature of the AGS is the behaviour of the spectrum in the +1st order, in which the spectral range is limited by the so-called cut-off wavelength $\lambda_{\rm co}$ corresponding to the diffraction angle $\psi = 90°$:

$$\lambda_{\rm co} = d(1 - \sin\varphi). \qquad (30)$$

Since the inverse dispersion D^{-1} depends strongly on ψ, then at $\psi \to 90°$ it tends to zero, which leads to a sharp increase in the spectral resolution near the wavelength $\lambda_{\rm co}$. This feature can be effectively used for diagnostic purposes.

Let us give a specific example of the choice of AGS parameters, intended for applications in nanolithography. In this case, there arises the problem of recording a spectrum in the region of the working wavelength λ_0 with a maximum possible spectral resolution and of a spectrum in a very wide region up to $\lambda \approx 200$ nm. Let there be a diffraction grating ruled with a period of 3 μm (333 lines $\rm mm^{-1}$). For a maximum spectral resolution at the working wavelength $\lambda_0 = 13.5$ nm we choose the cut-off wavelength $\lambda_{\rm co}$ close to λ_0, for example, $\lambda_{\rm co} = 13.8$ nm. With this wavelength, we find the angle of incidence of the radiation on the grating [expression (30)]: $\varphi = 84.5°$. The spectral range $\lambda \leqslant 200$ nm determines the minimum diffraction angle in the –1st order ($\psi_{\rm min} = 68°$). We select a CCD detector, for example, an Andor DO-420 camera with a pixel size of 26×26 μm and a length of the sensitive part of 26.6 mm. We assume that the width of the detector's instrument function is equal to the width of 3 pixels, or 78 μm. To overlap the range of diffraction angles $\psi = 68–90°$ with this detector, $F \approx 60$ mm is needed, i.e., the spectrometer can be very compact. We assume that the grating is located in the immediate vicinity of the entrance slit ($f = 4$ mm). With the help of the formulas given above, we find the spectral resolution $\delta\lambda$, determined by various factors (Figs 7, 8) and the spectral resolving power $\lambda/\delta\lambda$ for different values of s and A (Table 2). It follows from Table 2 that at the wavelength $\lambda_0 = 13.5$ nm

Table 2. The spectral resolving power ($\lambda/\delta\lambda$) of an AGS for various widths of the entrance slit s and distances A for wavelengths $\lambda_0 = 13.5$ nm (+1st diffraction order) and 100 nm (–1st order). The source size is $\theta = 0.4$ mm.

s/mm	A/mm 500		1000		2000	
	13.5 nm	100 nm	13.5 nm	100 nm	13.5 nm	100 nm
0	0	0	0	0	0	0
0.05	54	44	90	44	121	44
0.08	56	30	99	30	145	30
0.1	56	25	101	25	152	25
0.2	56	13	104	13	160	13

(+1st order), it is possible to achieve $\lambda/\delta\lambda \approx 150$, which is quite sufficient for recording the structure of the spectrum in the region of the working wavelength. In this case, the spectral resolution depends mainly on the angular size of the source (see Fig. 7). At $\lambda = 100$ nm, in the –1st order, the spectral resolution $\lambda/\delta\lambda$ is 20–40, is determined by the width of the input slit (the case of the so-called point source) and is virtually independent of the angular size of the source (Fig. 7).

The above estimates showed that the AGS with one diffraction grating can simultaneously solve two seemingly mutually exclusive problems: to record the spectrum in a wide range with a low spectral resolution and to record the spectrum in a narrow range with a much higher resolution (Fig. 8). We will show that the solution of these problems with the help of the TGS requires the use of at least two gratings. To do this, we will perform a numerical simulation of the spectra registered by the AGS and TGS. We will assume that the initial spectrum consists of six spectral lines (Fig. 9a) in the wavelength range 13.5–200 nm with the same intensity $I_i = 1$ and width $\delta\lambda_i = \lambda_i/200$. For simplicity, in both spectrometers, the efficiency of the gratings and CCD detectors is equal to unity. In this case, the intensity I of the lines in the spectrum will be determined by the devices' instrument function: $I = I_i\delta\lambda_i/\delta\lambda$, i.e. the better the spectral resolution $\delta\lambda$, the higher the line intensity. For an adequate comparison of the intensities recorded by the spectrometers, we will use the same parameters: $s = 0.05$ mm, $A = 1000$ mm, $F = 60$ mm, $\theta = 0.4$ mm, detector length 26.6 mm. The intensity of the lines is shown in Fig. 9b for two diffraction orders in the AGS with one 333 lines mm^{-1} diffraction grating. We determine the parameters of the transmission gratings so that the spectral resolution at $\lambda_0 = 13.5$ nm and the recording range are the same as those for the AGS. For the first condition, we require a grating with at least 12000 lines mm^{-1}, but the spectral range is bounded from above by a wavelength of 37 nm (TGS1, Fig. 9c). For the spectrum to be detected in the range up to 200 nm, a 2000 lines mm^{-1} grating (TGS2, Fig. 9d) is required; in this case, at $\lambda_0 = 13.5$ nm, the spectral resolution is $\lambda/\delta\lambda = 13.5$. The intensity ratio ($I_{max}/I_{min}$) in the spectral range 13.5–200 nm in this case is 2.5 for the AGS and 7.3 for the TGS2. Thus, the AGS less distorts the intensity ratio in the spectrum than the TGS2.

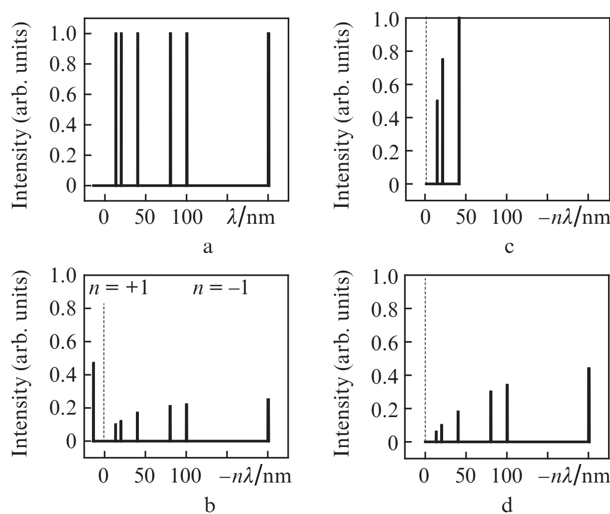

Figure 9. Results of numerical simulation of the spectra recorded by the AGS and TGS: (a) the initial spectrum; (b) the spectrum recorded by the AGS with a 333 lines mm^{-1} grating in the +1st and –1st diffraction orders; (c, d) spectra recorded by the TGS with 12000 and 2000 lines mm^{-1} gratings, respectively. The zero-order position is marked with a dotted line.

Let us consider some aspects of AGS applications. Due to the flat relief of the amplitude grating, the reflection is observed in a wide spectral range, but the main energy is concentrated in the zeroth order. This circumstance leads to a drop in the light intensity of the device, and so its use is particularly reasonable for intense radiation sources. As follows from Table 2, the spectral resolving power in the +1st order strongly depends on the angular size of the source. This leads to an additional requirement, i.e. a small ($\theta/A \leqslant 10^{-3}$ rad) angular size of the source, which is easily fulfilled if the radiation source is intended for nanolithography.

The AGS can have very small sizes (length ~100 mm with the detector), which allows it to be installed both at a long distance from the source and (if necessary) inside a vacuum chamber.

As mentioned above, to completely suppress the reflection in even diffraction orders, it is necessary that the ratio of the widths of the reflecting and non-reflecting parts of the grating be 1 : 1. Even small deviations from this condition lead to the appearance of even orders in the spectrum. In addition, there are odd diffraction orders in the spectrum. Allowance for the multiple overlap of higher diffraction orders can be carried out using various mathematical methods (see, for example, [22, 23]).

The AGS parameters strongly depend on the angle of incidence φ of radiation on the grating. To align the spectrometer, an additional focusing unit is needed, the use of which makes it possible not only to fine-adjust the angle φ, but also to centre the path of the rays in a plane perpendicular to the dispersion direction. This allows one to minimise the influence of the possible curvature of the spectral lines on the spectral resolution.

A particular disadvantage of the AGS scheme is the location of the diffraction grating directly behind the entrance slit, which can lead to contamination of the grating by the plasma source products. To protect the spectrometer, one can use mechanical and electromagnetic shutters, magnetic shielding, buffer gas, etc. Such methods are being successfully developed also in nanolithography to protect collimators [2].

The luminosity of the instrument and its absolute calibration are separate questions. Absolute measurements require absolutely calibrated radiation detectors, and for the known device geometry it is necessary to know the efficiency of the grating reflection. The efficiency of the grating is usually calculated theoretically, and carrying out this calculation in principle is possible both for the transmission grating and for the reflection grating. Thus, for the TGS in the short-wavelength range of the spectrum, the grating efficiency is practically independent of the wavelength. Difficulties in calculations arise on the long-wavelength part of the spectrum with $\lambda \geqslant 100$ nm due to a deviation from the ideal geometry of the grooves, and also because of uncertainty in the values of the optical constants. We hope that the flat relief of the amplitude grating with a small roughness made of a material with known optical constants and thickness of the reflecting part of the grooves will make it possible to reliably calculate the reflection coefficient. In addition, its installation in a grazing incidence scheme can simplify the theoretical calculations of the reflection coefficient of the grating and increase it in the

short-wavelength range of the spectrum. Unfortunately, the calculation of the grating efficiency in the entire spectral range is a difficult task, which is beyond the scope of this paper and requires separate consideration.

In conclusion, we note once again the main properties of the new scheme of a compact VUV grazing incidence spectrometer based on a plane amplitude grating. Such a spectrometer is effective in the study of intense radiation sources with a small angular aperture. The spectrometer allows simultaneous detection of spectra at the +1st order edge of diffraction with a sufficiently high spectral resolution $\lambda/\delta\lambda \sim 100-150$), and in the –1st order with a moderate resolution ($\lambda/\delta\lambda \sim 15-30$), but in a very wide spectral range (5–200 nm). The reflection coefficient of the amplitude grating calculated in advance and the use of an absolutely calibrated CCD detector will allow absolute (quantitative) measurements of the intensities in these spectral ranges.

Acknowledgements. The author is grateful to A.V. Mitrofanov for valuable remarks, to O.F. Yakushev for help in the work, to V.V. Medvedev and V.M. Krivtsun for useful discussions. The work was partially supported by the Russian Foundation for Basic Research (Grant No. 02-15-04411).

References

1. Attwood D. *Soft X-rays and Extreme Ultraviolet Radiation. Principles and Applications* (New York: Cambridge Univ. Press, 2007).
2. Bakshi V. (Ed.) *EUV Sources for Lithography* (Bellingham, Washington: SPIE Press, 2006).
3. Wu B., Kumar A. *J. Vac. Sci. Technol.*, **B25**, 1743 (2007).
4. Fujioka S., Nishimura H., Nishihara N., Miyanaga N., Izawa Y., Mima K., Shimada Y., Sunahara A. *Plasma Fusion Res.: Rev. Articl.*, **4**, 048 (2009).
5. Banine V.Y., Koshelev K.N., Swinkels G.H.P.M. *J. Phys. D: Appl. Phys.*, **44**, 253001 (2011).
6. Fomenkov I.V., La Fontaine B., Brown D., et al. *J. Micro/Nanolith. MEMS MOEMS*, **11**, 021110 (2012).
7. Schopper H.W., Van Speybroeck L.P., Delvaille J.P., Epstein A., Källne E., Bachrach R.Z., Dijkstra J., Lantward L. *Appl. Opt.*, **16** (4), 1088 (1977).
8. Edmann K., Kishimoto T., Herrmann P., Mizui J., Pakula R., Sigel R., Witkowski S. *Laser Part. Beams*, **4** , 521 (1986).
9. Wilhein T., Rehbein R., Hambach D., Berglund M., Rymell L., Hertz H.M. *Rev. Sci. Instrum.*, **70**, 1694 (1999).
10. Weaver J.L., Holland G., Feldman U., Seely J.F., Brown C.M., Serlin V., Deniz A.V., Klapisch M. *Rev. Sci. Instrum.*, **72**, 108 (2001).
11. Bergeson S., Gray N., Harrison M., Knight L., Yakushev O., Shevelko A. *Workshop Agenda and Abstracts of 2008 Intern. Workshop on EUV Lithography* (Maui, Hawaii, June 10–12, 2008) p. 38.
12. Goh S.J., Bastiaens H.J.M., Vratzov B., Huang G., Bijkerk F., Boller K.J. *Opt. Express*, **23**, 4421 (2015).
13. Fuchs S., Rödel C., Krebs M., Hädrich S., Bierbach J., Paz A.E., Kuschel S., Wünsche M., Hilbert V., Zastrau U., Förster E., Limpert J., Paulus G.G. *Rev. Sci. Instrum.*, **84**, 023101 (2013).
14. Basov N.G., Zakharenkov Yu.A., Rupasov A.A., Sklizkov G.V., Shikanov A.S. *Diagnostika plotnoi plazmy* (Diagnosis of A Dense Plasma) (Moscow: Nauka, 1989) Ch. 5, pp 162–167.
15. Palmer E.W., Hutley M.C., Franks A., Verrill J.F., Gale B. *Rep. Progr. Phys.*, **38**, 975 (1975).
16. Malyshev V.I. *Vvedenie v eksperimental'nuyu spektroskopiyu* (Introduction to Experimental Spectroscopy) (Moscow: Nauka, 1979).
17. Zaidel' A.N., Shreider E.Ya. *Vakuumnaya spektroskopiya i ee primenenie* (Vacuum Spectroscopy and Its Application) (Moscow: Nauka, 1976).
18. Vinogradov A.V. (Ed.) *Zerkal'naya rentgenovskaya optika* (X-ray Mirror Optics) (Leningrad: Mashinostroenie, 1989) p. 249.
19. Compton A.H., Doan R.L. *Proc. Natl. Acad. Sci.*, **11**, 598 (1925).
20. Bäcklin E. *Zs. F. Phys.*, **93**, 450 (1935).
21. Siegbahn M., Magnusson T. *Zs. F. Phys.*, **62**, 435 (1930).
22. Kazakov E.D., Shevelko A.P. *Vopr. At. Nauki Tekh., Ser. Termoyad. Sintez*, **37**, 71 (2014).
23. Kologrivov A.A., Rupasov A.A., Sklizkov G.V. Preprint FIAN No. 2 (Moscow, 2017).